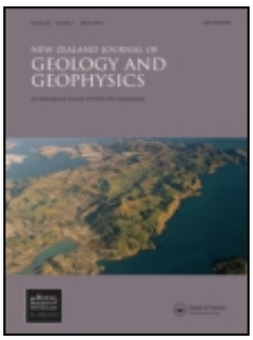

New Zealand Journal of Geology and Geophysics

ISSN: 0028-8306 (Print) 1175-8791 (Online) Journal homepage: https://www.tandfonline.com/loi/tnzg20

Volcanism, structure, and petrology of the Whiritoa-Whangamata coastal section, Coromandel Volcanic Zone, New Zealand: Facies model evidence for the Tunaiti caldera

R. M. Briggs & B. W. J. Fulton

To cite this article: R. M. Briggs & B. W. J. Fulton (1990) Volcanism, structure, and petrology of the Whiritoa-Whangamata coastal section, Coromandel Volcanic Zone, New Zealand: Facies model evidence for the Tunaiti caldera, New Zealand Journal of Geology and Geophysics, 33:4, 623-633, DOI: 10.1080/00288306.1990.10421380

To link to this article: https://doi.org/10.1080/00288306.1990.10421380

New Zealand Journal of Geology and Geophysics, 1990, Vol. 33: 623–633
0028–8306/90/3304–0623 $2.50/0

Volcanism, structure, and petrology of the Whiritoa–Whangamata coastal section, Coromandel Volcanic Zone, New Zealand: facies model evidence for the Tunaiti caldera

R. M. BRIGGS
B. W. J. FULTON
Department of Earth Sciences
University of Waikato
Private Bag 3105
Hamilton, New Zealand

Abstract Coastal sections between Whiritoa and Whangamata, eastern Coromandel, New Zealand, have exposed a Late Miocene volcanic and pyroclastic sequence which has been interpreted using a caldera facies model. The present-day coastline transects the middle of the caldera, which has been named here the **Tunaiti caldera**. The sequence comprises: (1) precaldera andesite and dacite lavas; (2) caldera-forming dacitic eruptions and interbedded plinian tuffs; (3) a variety of tilted and deformed moat deposits including extrusive and intrusive preresurgent rhyolitic volcanics, diatomaceous lake sediments, and postcollapse mesobreccias; (4) intracaldera resurgent biotite rhyolite domes and flows; (5) postcaldera dikes and lavas of hornblende rhyolite; and terminated with (6) postcaldera dacite lavas. There is a trend in composition with time from early andesites and dacites through to voluminous intracaldera rhyolites, which reverted to less silicic, small volume ring-fracture rhyolites and dacites. Incompatible element ratios between the andesites, dacites, and rhyolites indicate that they have not been derived from a single evolving magma chamber. The andesites have compositions (low Nb, high Ba/La) typical of subduction-related magmas, and these magmas ascended to upper crustal levels where they mixed with discrete rhyolitic magmas beneath the caldera to produce the dacites. Hydrothermal alteration or mineralisation associated with the caldera is unknown. A caldera facies model approach could be a useful tool in the future for recognising eroded ancient calderas in Coromandel and Tauranga, and possibly also for locating associated epithermal or subaqueous volcanogenic exhalative massive sulphide mineralisation.

Keywords Coromandel Volcanic Zone; Whiritoa; Whangamata; Late Miocene; volcanic rocks; calderas; geochemistry; petrology; andesites; dacites; rhyolites; magma mixing

INTRODUCTION

Rhyolitic calderas can be recognised on the basis of many features including: (1) thick intracaldera ignimbrites and co-ignimbrite breccias, and thin outflow sheets which may show a radial distribution; the ignimbrites may be intercalated with pyroclastic fall deposits; (2) late-stage rhyolite domes and flows which lie within or at the margins of the caldera, forming intracaldera complexes or arcs of domes along ring fractures, although some may be erupted outside the main caldera rim; (3) a variety of caldera-fill or moat deposits that lie between the intracaldera rhyolite lavas and the caldera wall—for example, lake and fluvial epiclastic sediments, caldera-collapse or postcollapse breccias from erosion or collapse of the caldera wall, and localised lenses of bedded or massive sulphides; (4) geophysically defined subcircular basement depressions, shown for example by subcircular negative gravity anomalies produced by caldera-infill with lower density pyroclastic rocks; (5) hydrothermal systems including epithermal mineral deposits; and (6) circular or arcuate structures observed by remote sensing techniques. Some or all of these features can be combined to form a caldera facies model that can be used to identify ancient calderas in the geologic record (Cas & Wright 1987).

We have used such a caldera facies model approach to identify an eroded Late Miocene caldera, which we have named the **Tunaiti caldera**, on the eastern side of the Coromandel Peninsula, New Zealand (Fig. 1). This paper describes a sequence of outflow ignimbrites with intercalated plinian fall deposits, late-stage intracaldera rhyolite domes and flows, a caldera rim fault, a variety of moat deposits including lake sediments and postcollapse breccias, and an arcuate structure observed in the topography which coincides with a magnetic anomaly high. This sequence is well exposed in coastal outcrops between Whangamata and Whiritoa.

Skinner (1986) mapped six main areas of major explosive rhyolitic volcanism in the Coromandel Volcanic Zone, and has recognised caldera structures associated with three of them based on circular patterns on landsat images and geophysical data. However, previous work on the complex volcanic rocks of the Coromandel Peninsula has mainly concentrated on stratigraphic approaches; the facies model approach to elucidate the relationships between volcanic and pyroclastic units has not been previously attempted.

Rhyolite domes and flows in the presently active Taupo Volcanic Zone to the southeast of Coromandel are always associated with calderas, and generally restricted to intracaldera or caldera rim locations, or at least are never located far outside the caldera rim. By this analogy alone, the abundant Miocene–Pliocene rhyolite domes and flows of eastern Coromandel and in the area extending south to Tauranga and Matamata, are likely to be associated with eroded caldera structures.

Active or recently active rhyolite calderas like those of Taupo Volcanic Zone have been recognised on the basis of

G90008
Received 7 March 1990; accepted 20 July 1990

such features as classically exposed, circular, partially lake-infilled basinal structures, rhyolite dome and flow complexes and ring fractures, and subcircular negative gravity anomalies (Rogan 1982; Wilson et al. 1984). However, in many instances in other Tertiary calderas in the western U.S.A., the calderas become topographically inverted with age, and any original negative gravity anomaly tends to be obliterated with such inversion and uplift. It is possible that topographic inversion of older Miocene calderas has also occurred in some Coromandel examples, and residual gravity anomaly maps may not be so valuable for recognising calderas as they are in Taupo Volcanic Zone. Hence we believe that a caldera facies model approach is the best method, and should provide a sound basis in the future for recognising eroded calderas in Coromandel and Tauranga.

In this paper we also report preliminary petrologic data including some major and trace element geochemistry. Previous petrologic data from this area are unknown, except for a single whole-rock analysis in Rutherford (1976).

GEOLOGIC SETTING

Tunaiti caldera is located on the east coast of Coromandel Peninsula, between Whiritoa and Whangamata (Fig. 1). It forms part of the Whitianga Group of Late Miocene – Early Pleistocene age, which is included in the Coromandel Volcanic Zone of Skinner (1986). The Whitianga Group is described by Moore (1983) and Skinner (1986) as consisting of rhyolite dome complexes, lava flows, ignimbrite, fall deposits, and epiclastic sediments. However, the geochemistry of these complex rocks is not well known, and we describe here rocks with more diverse compositions including andesites and dacites. Age constraints on the various volcanic episodes within the Whitianga Group are poor and are summarised in Skinner (1986). Rutherford (1978), Skinner (1986), and Seward & Moore (1987) demonstrated that there appeared to be a general trend of rocks younging to the south in the Coromandel Volcanic Zone. There are no age data on any rocks associated with the Tunaiti caldera, although K-Ar dating is in progress. A fission-track age of 7.21 ± 0.84 Ma on rhyolite lavas at Onemana just north of Whangamata (Seward & Moore 1987) provides the geographically closest age data, and the rocks of the Tunaiti caldera probably have a similar age, based on analogous degrees of erosion.

The six major explosive volcanic centres recognised by Skinner (1986) for the Whitianga Group are: (1) south of Whitianga; (2) west of Tairua; (3) northwest of Whangamata; (4) Waihi basin; (5) Tauranga–Te Puke; and (6) southeast of Matamata (Fig. 1). Skinner (1986) also recognised three calderas, based partly on landsat images and partly on magnetic and gravity anomalies (Woodward 1971; Hunt & Syms 1977): west of Tairua—named the Kapowai caldera; northwest of Whangamata—named the Wharekawa caldera; and the Waihi caldera centred on the Waihi basin. However, Skinner (1986) also pointed out that there could be calderas in the Whitianga area and the Mercury Islands based on structural rings of rhyolite domes and geophysical data.

By analogy with the calderas of the Taupo Volcanic Zone (Wilson et al. 1984) and well-described caldera complexes elsewhere (e.g., in continental western U.S.A.—Smith et al. 1961; Ratté & Steven 1967; Lipman 1975, 1976, 1984; Bailey et al. 1976; Christiansen 1979, 1984), we consider it likely that there are calderas associated with each of the six major explosive

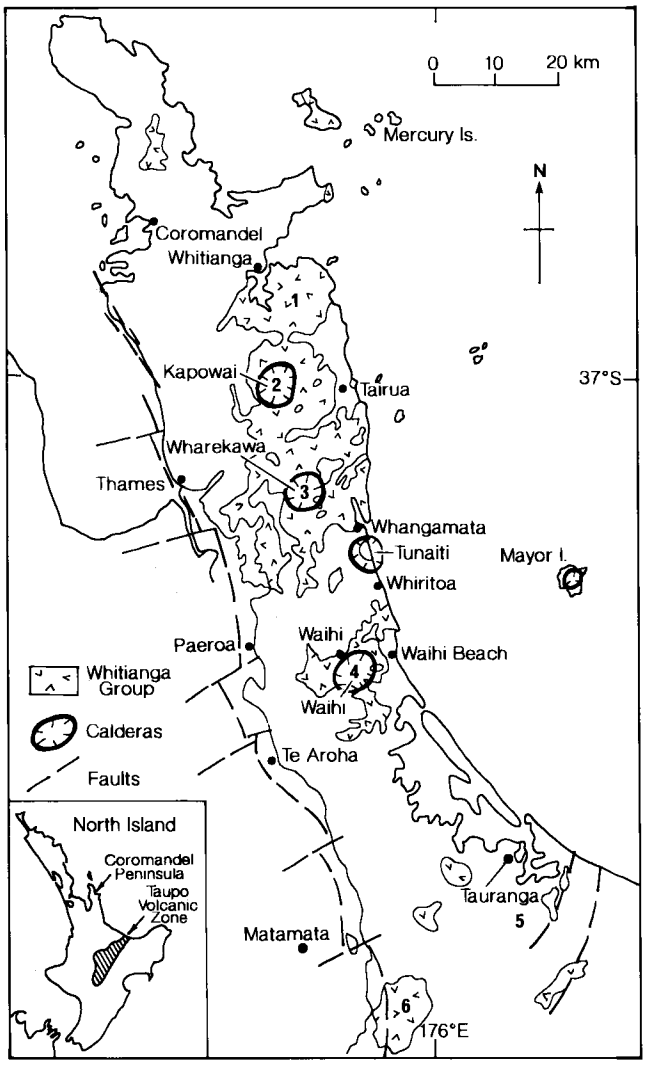

Fig. 1 Map of Coromandel Volcanic Zone, showing the distribution of Whitianga Group and associated calderas, based mainly on maps and descriptions in Skinner (1986). Tunaiti caldera is identified in this study. Faults of the Hauraki Rift are after Hochstein & Nixon (1979).

volcanic centres of eastern Coromandel. Furthermore, some of these volcanic centres or volcanic fields could contain multiple nests or clusters of closely associated or overlapping calderas with complex caldera geometry, as seen for example in the San Juan Mountains, Colorado (Lipman 1984), and Yellowstone, Wyoming (Christiansen 1984).

The Tunaiti caldera is probably a subcircular structure and is about 5 km in diameter (Fig. 2). The eastern half of the caldera has been completely eroded, and the present-day coastline transects the middle of the caldera. Only the south wall of the caldera is exposed, and none of the caldera wall has any topographic expression. Intracaldera rhyolite dome lavas form the highest point of the structure, and reach an elevation of 221 m at Tunaiti Trig, after which the caldera has been named. Inland exposures are poor and are capped by late Quaternary tephras derived from the Taupo Volcanic Zone and Mayor Island (cf. Hogg & McCraw 1983). However, the western half of the subcircular structure of the caldera is sharply delineated by low-altitude aerial, high resolution, colour-contoured maps of magnetic intensity (unpubl. data,

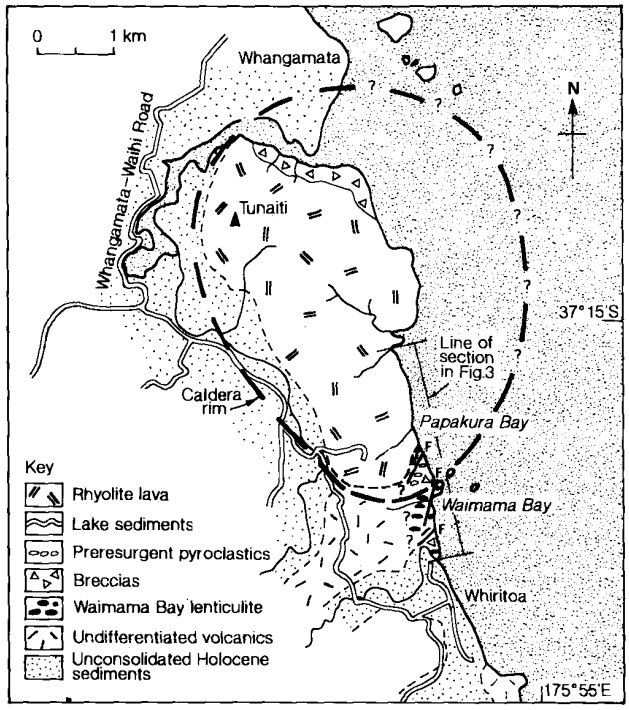

Fig. 2 Geological map of the Whiritoa–Whangamata area, eastern Coromandel, showing the location of the Tunaiti caldera.

G. J. Jones pers. comm. 1990). We have generously been able to use this unpublished data to define the inland caldera rim where exposures are poor or absent. The delineation of the eastern half is of course unknown.

VOLCANIC SEQUENCE

A summary of the six main episodes of volcanic activity of the Tunaiti caldera is given in Table 1. It is not possible to estimate erupted volumes and to determine magma supply rates of any of the eruptive events because of the marked erosion of these rocks. Marine erosion in eastern Coromandel Peninsula is relatively rapid; inland rocks are generally deeply weathered to clays, and good exposures are almost totally confined to the coast.

A volcanic structural section is shown in Fig. 3 with a diagrammatic sequence of volcanic events given in Fig. 4. Major and trace element geochemical data for representative rocks from each of the main volcanic events are in Table 2. Further petrographic details and mineralogical compositions are given in Fulton (1988).

1. Precaldera lavas

The earliest volcanic rocks in the Whiritoa–Whangamata section are andesitic and dacitic lavas and autoclastic breccias. We argue later that these lavas played the initial role in the petrologic evolution of the volcanic sequence, and interpret them as representing early flows flanking the incipient caldera ring fractures. They show no signs of hydrothermal alteration and are hence not regarded as belonging to the older Miocene Coromandel Group rocks.

The precaldera andesitic and dacitic lava flows are intercalated with ignimbrites, fall deposits, and autoclastic breccias. The andesites (55% SiO_2) are porphyritic or glomeroporphyritic and contain phenocrysts of calcic plagioclase (An_{63-85}), hypersthene (En_{71-77}), minor titanomagnetite and ilmenite, set in a fine-grained intersertal groundmass. The dacite lavas (63–65% SiO_2) are highly porphyritic; phenocrysts include plagioclase (An_{44-61}), hypersthene (En_{60-64}), augite, amphibole (edenite to edenitic hornblende compositions), biotite, quartz, titanomagnetite, and ilmenite.

2. Outflow sheets

The main caldera-forming eruptive unit we have recognised produced extensive outflow sheets, and is informally named here the Waimama Bay lenticulite. The lenticulite is best exposed in Waimama Bay where it reaches 35 m in thickness, but it is deeply eroded and the stratigraphic lower and upper contacts are not exposed. The apparent base of the lenticulite is lithic rich, with lithics comprised of dacites, andesites, and rhyolites. The lenses are dense, nonvesicular, vary from 1 to 30 cm in length and up to 8 cm in thickness, and have a dacitic (65% SiO_2) composition. The lenses are abundant (up to 25%) and strongly orientated. However, in contrast to the rest of the lenticulite, some of the lenses lack hornblende and provide evidence that the lenticulite is a mixed rock composed of lenticular clasts surrounded by a matrix which, in some cases, differs mineralogically.

Crystals in the lenticulite constitute 38–48 modal percent. Further evidence of mixing is provided by both plagioclase (An_{40-70}) and hypersthene (En_{60-77}), which show wide but evenly spread compositional variations, and normal and reverse zoning. The compositional variations overlap with the compositional fields characteristic of these minerals in andesites and rhyolites. Other matrix crystals include augite, hornblende, biotite, quartz, titanomagnetite, and ilmenite. Interstitial fine-grained devitrified glass and chloritic material also occurs, but shard textures are lacking.

We have used the term "lenticulites" in a textural sense because they appear to be varieties of andesitic to dacitic ignimbrites which contain abundant orientated lenses. However, we are not certain whether they have a pyroclastic flow origin and are in fact ignimbrites, or if they are spatter-fed lava flows. Whichever, the term "lenticulites" is considered to be the most appropriate.

The dacitic composition of the Waimama Bay lenticulite is surprising because we would expect that the main caldera-forming eruption would have a composition broadly similar to

Table 1 Summary of volcanic activity of Tunaiti caldera, Coromandel Volcanic Zone.

Event	Volcanic activity and products
6.	Postcaldera andesitic to dacitic lavas (Omahine dacite)
5.	Postcaldera hornblende rhyolites—lavas and dikes
4.	Intracaldera resurgent biotite rhyolite dome lavas
3.	Moat deposits: (iii) postcollapse mesobreccias
	(ii) diatomaceous lake sediments and lignites
	(i) extrusive and intrusive pre-resurgent rhyolitic volcanism (deformed zone)
2.	Caldera-forming eruptions—dacitic lenticulite outflow sheets (Waimama Bay lenticulite) and interbedded plinian tuffs
1.	Precaldera andesitic and dacitic lavas, tuffs, autoclastic breccias.

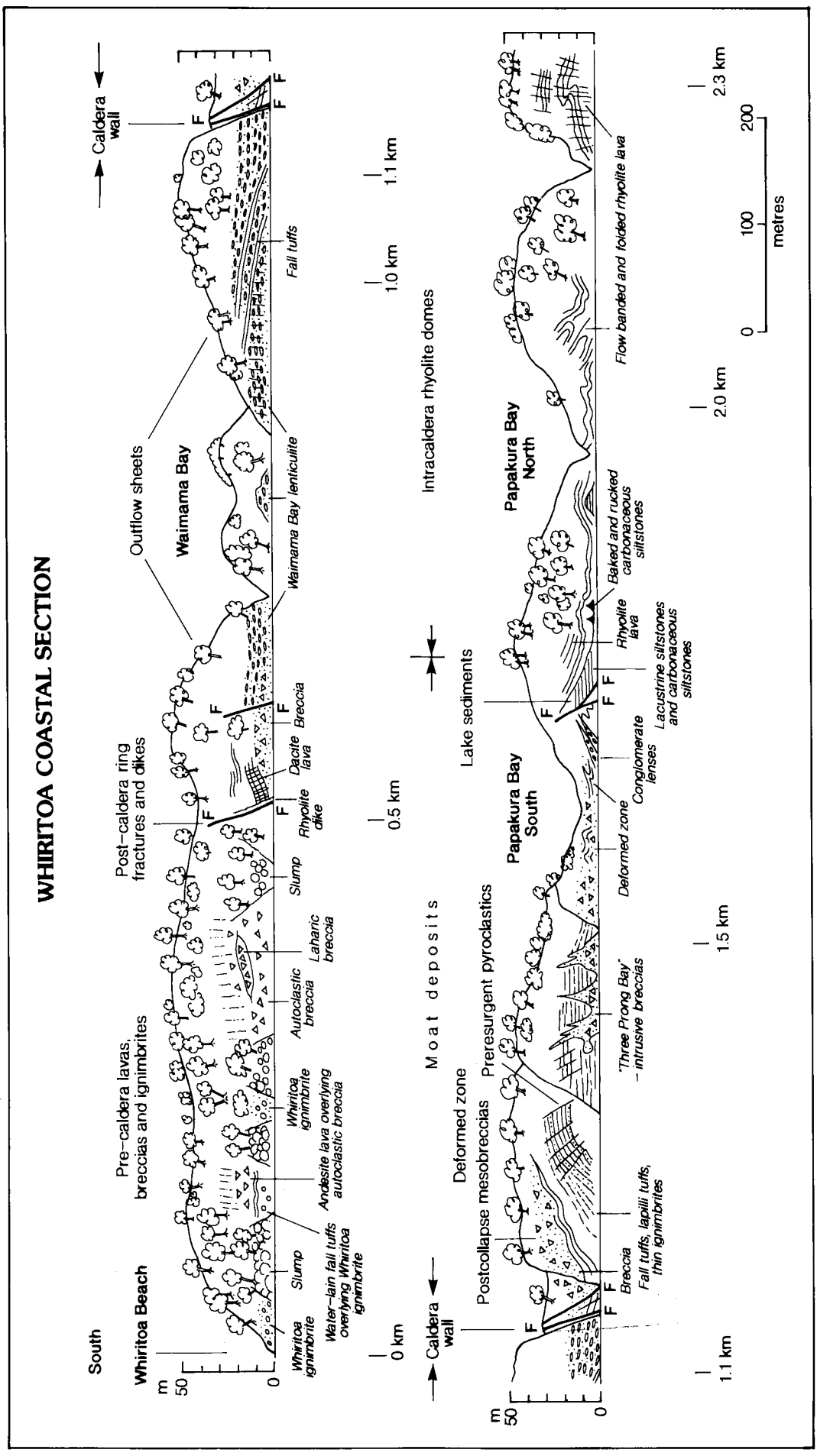

Fig. 3 Coastal section from Whiritoa Beach to Papakura Bay, Coromandel Volcanic Zone. Lithologies are given below the section, and the interpretation of the caldera facies is given above the section. (Refer to Fig. 2 for location.)

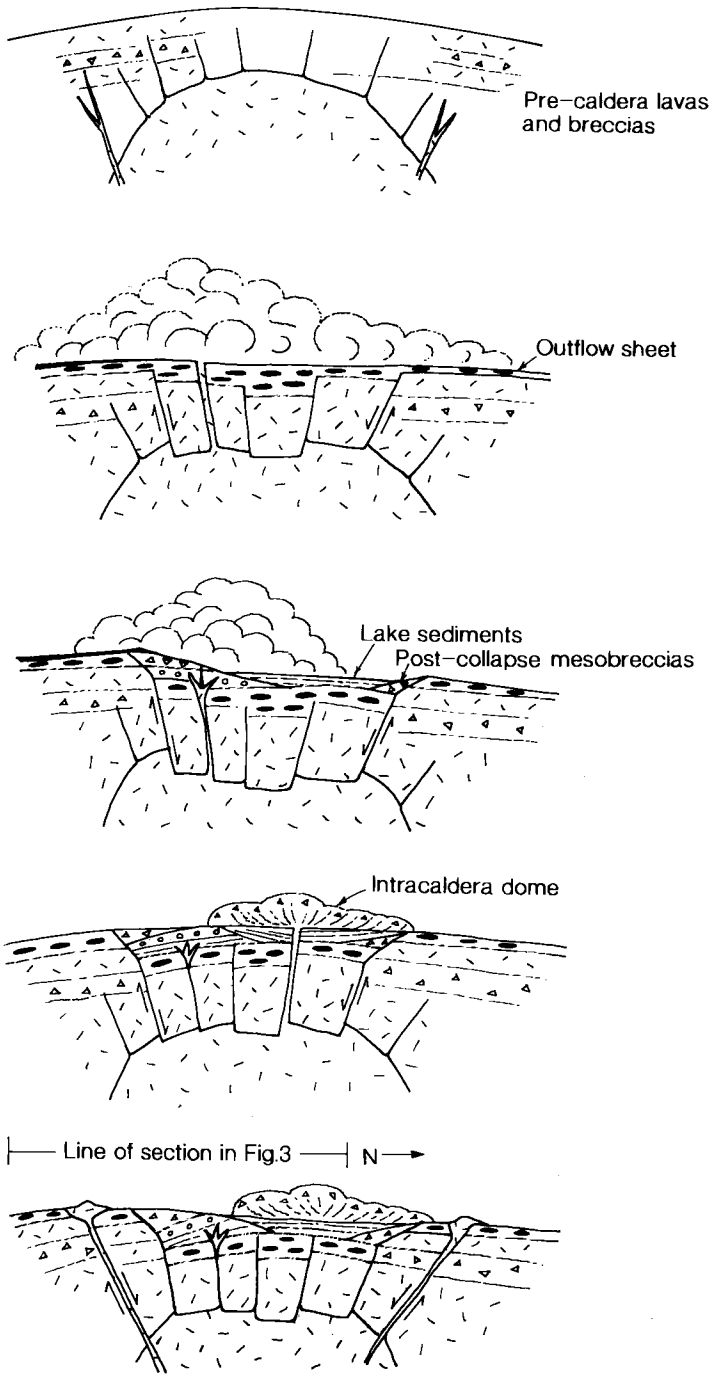

Fig. 4 Schematic diagrams showing the possible sequence of events in the development of the Tunaiti caldera, eastern Coromandel.

that of the later intracaldera resurgent rhyolitic dome lavas. However, rhyolitic ignimbrites have not been observed in the Whiritoa–Whangamata region, although it is likely that unwelded rhyolitic pyroclastic flows could have been erupted but are now either totally eroded or not exposed.

3. Moat deposits

As a result of the eruption of the Waimama Bay lenticulite, and possibly also other eruptives, the Tunaiti magma chamber was partially emptied and its roof consequently collapsed. Collapse probably took place along arcuate ring faults, and the major ring fault occurs just north of Waimama Bay (Fig. 2). However, displacement on this fault, interpreted to be the main caldera wall, cannot be measured and it has no topographic expression inland. The north wall of the caldera is not exposed but is considered on the basis of the magnetic anomaly map to cut across the southern part of Whangamata Beach. Most of the caldera was later filled with thick rhyolite dome lavas, and the rocks in the region between the caldera wall and the intracaldera rhyolite lavas are collectively termed the "moat deposits".

The moat deposits consist of a complex sequence of pyroclastic deposits, postcollapse breccias adjacent to the caldera wall, and lake sediments with interbedded lignites. The moat deposits are in places highly deformed, and show steep dips, numerous small-scale faults, possible complex volcanic intrusive relations, and syndepositional soft-sediment deformational structures including recumbent folding.

Table 2 Major (wt% normalised to 100% volatile-free) and trace element (ppm) XRF analyses of Tunaiti caldera eruptives and associated rocks.

	Precaldera lavas													Postcaldera lavas	
	Andesites		Dacites		Waimama Bay lenticulite			Moat rhyolite	Intracaldera biotite rhyolite dome lavas					Hornblende rhyolite	Omahine dacite
Sample no.	44	15	81	16	18	76	12	14	27	88	67	28	63	17	26
SiO_2	55.09	55.37	63.25	64.86	65.49	65.62	65.70	73.15	74.84	76.56	76.28	76.77	76.56	71.60	63.83
TiO_2	0.85	0.79	0.61	0.54	0.59	0.55	0.60	0.24	0.25	0.16	0.14	0.14	0.13	0.36	0.53
Al_2O_3	20.52	19.62	17.18	16.56	16.68	16.30	17.11	14.35	13.95	14.38	13.03	13.28	12.88	14.57	15.76
Fe_2O_3	1.49	1.49	1.15	0.95	1.00	0.98	1.00	0.38	0.46	0.36	0.32	0.33	0.28	0.56	1.00
FeO	5.96	5.97	4.60	3.80	3.93	3.73	4.01	1.53	1.84	1.45	1.29	1.33	1.13	2.25	3.98
MnO	0.11	0.11	0.08	0.09	0.07	0.06	0.05	0.05	0.04	0.02	0.01	0.01	0.03	0.03	0.09
MgO	3.35	3.65	2.62	2.56	1.48	2.13	1.19	0.76	0.24	0.16	0.23	0.18	0.18	0.74	3.10
CaO	7.86	8.18	4.76	4.68	4.21	4.34	3.94	2.47	1.15	0.38	1.04	0.78	1.22	2.91	5.98
Na_2O	2.94	2.90	2.96	3.13	3.52	3.41	3.42	3.08	3.18	2.20	3.61	3.01	3.60	3.67	3.17
K_2O	0.89	1.03	2.02	2.18	2.29	2.33	2.30	3.70	3.72	4.06	3.85	3.95	3.79	2.94	1.98
P_2O_5	0.13	0.11	0.09	0.09	0.10	0.09	0.01	0.02	0.05	0.02	0.02	0.02	0.01	0.05	0.08
Fe_2O_3*	8.25	8.22	6.45	5.28	5.56	5.19	5.67	2.19	2.59	2.07	1.79	1.85	1.60	3.13	5.47
LOI*	1.81	1.42	1.98	1.66	2.83	2.34	3.73	4.10	2.54	2.54	1.41	1.76	2.96	1.60	0.60
Total*	100.06	100.17	99.03	99.64	99.04	100.09	100.02	99.58	99.56	98.37	99.59	99.72	99.36	99.67	99.74
Sc	25	27	21	16	17	15	17	4	5	5	5	5	3	8	17
V	194	199	130	134	99	108	99	29	22	13	13	13	13	49	111
Cr	8	13	63	43	35	34	46	3	<2	<2	<2	<2	<2	16	59
Ni	12	6	10	12	10	10	7	<2	<2	<2	<2	<2	<2	3	11
Cu	13	17	37	21	15	20	16	35	5	4	16	5	4	36	26
Zn	92	66	80	76	71	62	73	41	46	30	41	32	33	42	53
Ga	19	18	17	16	15	16	18	13	13	16	13	15	15	13	16
Rb	19	22	73	80	84	83	83	163	138	142	140	140	135	105	72
Sr	390	424	176	187	203	199	196	138	82	32	74	57	79	149	224
Y	120	18	28	64	24	23	16	16	99	21	53	24	24	14	19
Zr	85	88	117	125	138	132	134	123	140	133	125	123	116	143	117
Nb	3	3	4	4	4	4	5	6	7	7	6	7	5	5	4
Ba	265	281	431	493	524	492	555	800	690	614	676	659	659	701	459
La	175	12	23	44	18	16	12	21	113	18	34	24	23	18	12
Ce	41	27	26	43	33	31	28	34	46	36	47	41	47	35	26
Pb	9	5	12	11	13	12	15	16	18	19	20	18	20	14	10
Th	4	4	7	7	9	9	10	12	13	15	13	14	14	11	6
U	0.5	0.8	1.6	1.3	2.6	2.7	2.3	2.8	4.3	3.3	2.7	2.4	3	3.7	2
K/Rb	389	389	230	226	226	233	230	188	224	237	228	234	233	232	228
Rb/Sr	0.05	0.05	0.41	0.43	0.41	0.42	0.42	1.18	1.68	4.44	1.89	2.46	1.71	0.70	0.32
Ba/La	2	23	19	11	29	31	46	38	6	34	20	27	29	39	38

*Original values.

Fe_2O_3 and FeO are recalculated values assuming $Fe_2O_3/(Fe_2O_3 + FeO) = 0.2$.

(i) Preresurgent moat volcanism

Volcanic activity continued after caldera collapse with the eruption of a complex sequence of rhyolitic (73% SiO_2) fall deposits, volcanic breccias, and thin (2 m) ignimbrites which have a total stratigraphic thickness of about 40 m and a lateral extent of over 200 m. Towards the southern part of the moat deposits section, this pyroclastic sequence progressively increases in dip to the south at up to 52°. These steep dips are considered to have been imparted by later resurgent doming in the central part of the caldera. Hence this sequence is referred to in Fig. 3 as the "preresurgent pyroclastics".

The pyroclastic sequence is composed of a sequence of moderately to well-sorted crystal- and lithic-rich fall deposits and moderately to poorly sorted volcanic breccias, containing hornblende-biotite rhyolitic pumice as the dominant juvenile clast (sample 14, Table 2). Accretionary lapilli are abundant in some fall deposits, and bedding-sag structures are common. The large size of many pumice bombs and blocks (30 cm pumice blocks are abundant and reach up to 60 cm) and lithic clasts up to 1 m also suggest that the vent was proximal. Lithic clasts consist of obsidian, andesite, rhyolite, and lenticulite. The andesite lithics (e.g., sample 15, Table 2) have similar compositions to those of the andesitic precaldera lavas, and the lenticulite lithics appear to be derived from the Waimama Bay lenticulite.

The pyroclastic sequence appears to be intruded by three wedge-shaped intrusions at the southern end of Papakura Bay. The intrusions are composed of volcanic breccias containing a variety of juvenile and accessory clasts up to 1 m, including pumice, siltstone, sandstone, andesite, dacite, rhyolite, and lenticulite. Associated crystal-rich tuff "veins" appear to emanate from the margins of the breccias and intrude into the overlying rocks for up to 5 m. There is no evidence of baking or contact metamorphic effects on the margins of the intrusions, and some deposits form recumbent folds and large-scale flame-like structures typical of soft-sediment deformation. We are uncertain of the origin of these unusual bodies, but consider they may be incipient volcanic intrusive structures that were probably deposited subaqueously while warm. Alternatively, they could have sedimentary contacts and represent cut and fill structures, where the preresurgent pyroclastics eroded or cut down into the underlying breccias and then infilled hollows (P. R. Moore pers. comm. 1990).

(ii) Lake sediments

Up to 10 m of lacustrine siltstones are exposed in a section along Papakura Bay, in fault contact with deformed moat pyroclastics to the south, and stratigraphically overlain by intracaldera rhyolite lava flows to the north. The siltstones contain abundant carbonaceous material at the base and thin (3 cm) lignite layers. In places the siltstones are baked and rucked up by the overriding rhyolite lava flows. The asymmetry of the latter structures, together with orientation of flow folds in the rhyolite lava, has not been analysed here, but could provide information on flow directions. SEM examination of the siltstones has confirmed the presence of diatoms, including *Melosira* and *Suriella*, and occasional sponge spicules, but none of these are time diagnostic.

The presence of diatomaceous lake sediments up to 10 m in thickness implies that drainage within the caldera was blocked for a considerable time prior to resurgence and extrusion of intracaldera domes.

(iii) Postcollapse breccias

Postcollapse breccias occur as a wedge-shaped unit adjacent to the caldera wall ring-fracture. The breccias consist of at least four units which thin to the north, away from the caldera rim. They attain a total thickness of 40 m, are poorly sorted, and are clast supported with clasts up to 1 m of andesite, hornblende-biotite pumice, and siltstone. The term "postcollapse breccia" is used because these breccias may be of rock-fall or rock-slide origin and have occurred interlayered with younger caldera-filling volcanic and sedimentary sequences, as indicated by the presence of hornblende-biotite pumice and siltstone clasts. Slumping and sliding could have resulted from oversteepening of the caldera walls. They could also be classed as mesobreccias because most of the clasts are 1 m or less in diameter. They are not regarded as caldera-collapse breccias as defined by Lipman (1976) because they are not confined to breccias that were formed early and accumulated within a caldera contemporaneously with collapse, and are not interlayered with intracaldera ignimbrites (or lenticulites) that were erupted during caldera formation.

4. Intracaldera rhyolite dome lavas

The progressive tilting (up to 52°) and deformation of the moat deposits on the caldera floor is evidence that resurgent structural doming has taken place. Doming was also accompanied by extrusion and emplacement of the intracaldera rhyolite domes. These domes have largely infilled the caldera and have constructed the highest present-day topographic relief.

Intracaldera rhyolite lavas are continuously exposed from Papakura Bay northward to the southern end of Whangamata Beach (Fig. 2). Air-photo interpretation suggests that up to six domes may be present, and mineralogic and geochemical data (Table 2) suggest all the lavas have closely related compositions, and probably form a genetically related intracaldera dome complex. The lavas are flow banded, spherulitic, and often display intricate flow folds. Basal breccias are often exposed, especially on the northernmost coastal section, and the basal 5 m of rhyolite lava south of Papakura Bay is highly perlitic.

The intracaldera rhyolites (74–76% SiO_2) are porphyritic (19–46 modal %). Plagioclase is generally the dominant phenocryst phase, with lesser amounts of biotite, quartz, titanomagnetite, and ilmenite. Pyroxenes and amphiboles are notably lacking. Plagioclase phenocrysts range in composition from oligoclase to sodic andesine (An_{23-35}), normal zoning is common, and Mg:Fe ratios in biotite phenocrysts (up to 12 modal %) range from 1:0.9 to 2.8.

5. Postcaldera hornblende rhyolites

After resurgence and emplacement of the intracaldera biotite rhyolite dome lavas, hornblende rhyolites erupted probably along ring fractures outside but concentric with the main caldera wall. The hornblende rhyolites are petrographically and temporally analogous to the ring domes of the Valles Caldera, New Mexico (Smith & Bailey 1968; Doell et al. 1968) and the moat rhyolites of the Long Valley Caldera, California (Bailey et al. 1976), except in this case the postcaldera hornblende rhyolites are located outside the caldera wall. However, details of the stratigraphic relations of the hornblende rhyolites are uncertain, and they have been found only on a small unnamed island 0.5 km east of Waimama Bay.

Postcaldera hornblende rhyolites have lower silica contents (71% SiO_2) than intracaldera lavas, contain 29 modal % phenocrysts including plagioclase (20%), hornblende (6%),

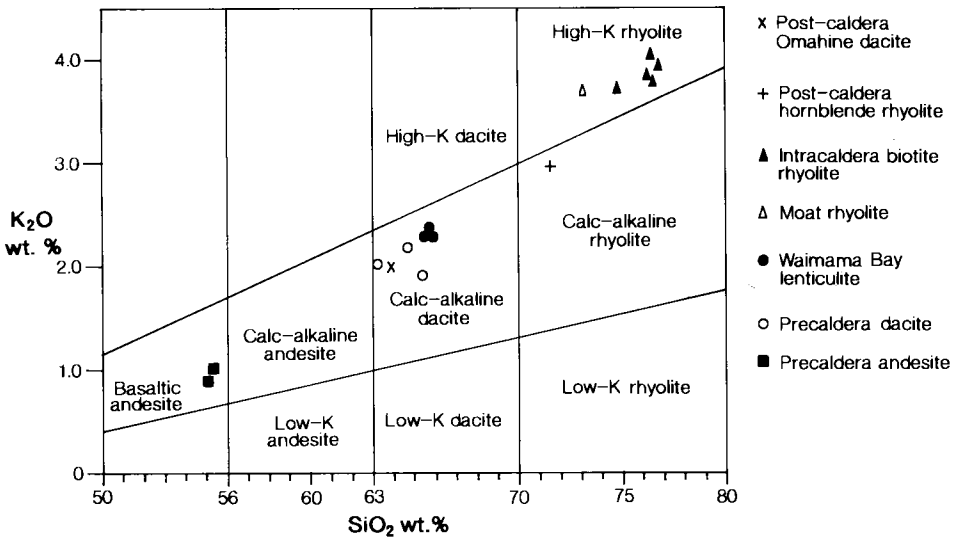

Fig. 5 K_2O versus SiO_2 (wt%, calculated on a 100% volatile-free basis) diagram for volcanic rocks associated with the Tunaiti caldera. Nomenclature after Ewart (1982) modified from Peccerillo & Taylor (1976).

and only minor biotite (0.4%), augite (0.4%), titanomagnetite, and ilmenite. Plagioclase phenocrysts (An_{43-50}) are more calcic relative to intracaldera lavas, and amphibole has edenite compositions. Fe-Ti oxide geothermometry data calculations (after Spencer & Lindsley 1981; Stormer 1982) indicate lower magmatic temperatures for postcaldera hornblende rhyolites (735°C) than either the moat biotite rhyolites (760°C) or intracaldera biotite rhyolites (755–860°C) (Fulton 1988).

6. Postcaldera Omahine dacites

Lava flows of Omahine pyroxene dacite (64% SiO_2) occur outside the caldera to the west. However, Skinner (1986) noted that these rocks, which are part of the Omahine Subgroup, have a close spatial relationship with the eastern Coromandel explosive volcanic centres. They occur as thick voluminous lava flows of andesitic or dacitic composition that are postcaldera in age, and appear to terminate the volcanic activity at each centre. Hence, some genetic relationship with caldera volcanism is implied, and this is supported by our data for Tunaiti caldera. Postcaldera Omahine dacite has a very similar composition to the precaldera dacite lavas and Waimama Bay lenticulite, and we argue in the next section that all of these dacites have a hybrid origin resulting from mixing of andesitic and rhyolitic magmas.

The Omahine dacite is dark grey, porphyritic or glomeroporphyritic, with abundant phenocrysts of plagioclase (An_{44-56}, 36 modal %), hypersthene (En_{60}, 5 modal %), augite (7 modal %), titanomagnetite and ilmenite (total opaques 10 modal %), set in an intersertal groundmass. Quartz and biotite are absent.

GEOCHEMISTRY AND MAGMA MIXING

The geochemical data (Table 2), and plots of K_2O versus SiO_2 (Fig. 5) and selected major and trace elements versus SiO_2 (Fig. 6), indicate that the rocks associated with the Tunaiti caldera fall into three distinct groups—basaltic andesites, dacites, and rhyolites—and that there are large compositional gaps between them. Moreover, Fig. 5 and 6 show that the dacites plot on linear trends intermediate between basaltic andesites and rhyolites, which suggests that the dacites may have been derived from mixing of basaltic andesite and rhyolite magmas. Linear trends occur for all elements except for small differences in Zr (see Fig. 6), and Ti and Cr abundances (not shown), which indicate that while mixing was possibly the dominant process, it was not the only process responsible for compositional variation of the suite. For example, these discrepancies could be explained by fractional crystallisation of magnetite (? with zircon inclusions) in either the basaltic andesites or rhyolites, subsequent to mixing. Quantitative mixing calculations suggest that a 50:50 mixing ratio of basaltic andesite : biotite rhyolite can produce the observed dacitic compositions. The interpretation that magma mixing has occurred is further supported by: (1) the wide range of phenocryst compositions in the dacites which overlap those in the basaltic andesites and rhyolites; (2) resorption and dusty textures of phenocrysts (cf. Sakuyama 1979); and (3) the wide range in temperature deduced from magnetite-ilmenite geothermometry. Fe-Ti oxide geothermometry indicates average temperatures of 760°C in the biotite rhyolites and 910°C in the basaltic andesites, which is the same temperature range determined from magnetite-ilmenite pairs in the dacitic lavas and lenticulites.

The rocks associated with the Tunaiti caldera show a progressive change in composition with time. The earliest precaldera volcanic rocks are basaltic andesite (55% SiO_2) varying to dacite (63–65% SiO_2) in composition, and are followed in the volcanic sequence by dacitic lenticulites (65% SiO_2), rhyolitic moat deposits (73% SiO_2), and intracaldera rhyolite domes (74–76% SiO_2). Postcaldera lavas then reverted to less silicic compositions with the eruption of 71% SiO_2 hornblende rhyolites, and finally terminated with the Omahine dacite (64% SiO_2).

These temporal compositional changes are not considered to have occurred in a single zoned magma chamber underlying the Tunaiti caldera which has evolved with time. Instead, the basaltic andesite and rhyolite magmas were discrete magmas which periodically mixed to produce the dacites. Evidence that the magmas are not genetically related to a single evolving zoned magma source is shown by the large differences in incompatible element ratios (e.g., K/Rb, Rb/Sr, Ba/La,Table 2) between the three groups, and the large compositional gaps. However, in rocks of these compositions that contain plagioclase and biotite phenocrysts, neither K/Rb nor Rb/Sr are truly incompatible element ratios, but if the rocks were

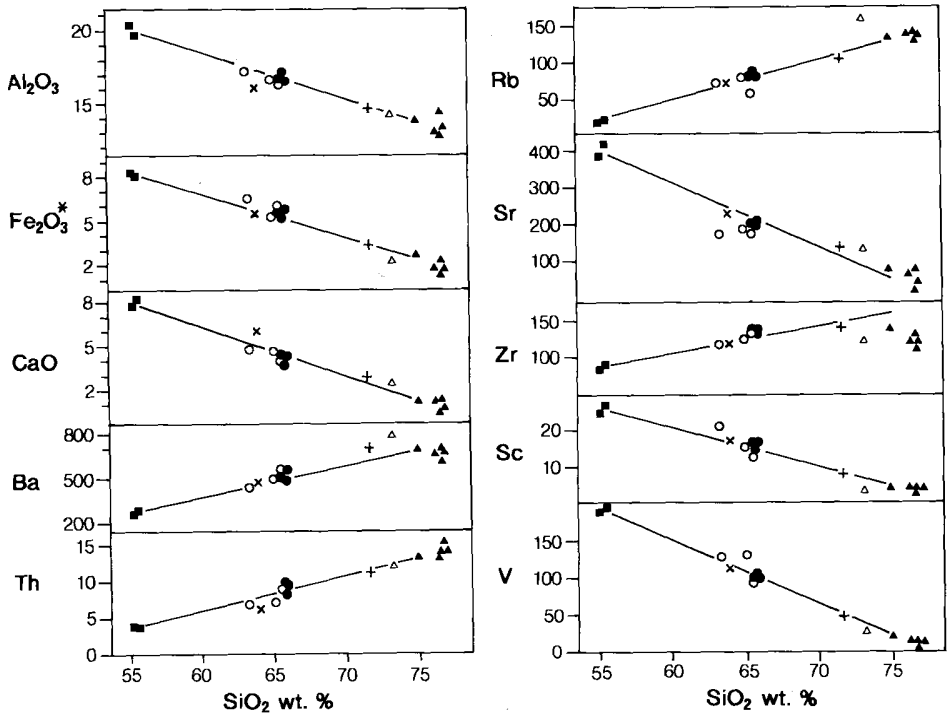

Fig. 6 Selected major element oxides (wt%) and trace elements (ppm) plotted versus SiO_2 for rocks associated with the Tunaiti caldera. Symbols as for Fig. 5. * Total iron reported as Fe_2O_3.

related to a single evolving magma source, then systematic and transitional trends in these element ratios would be expected. Although the distribution of individual volcanic vents is largely unknown, in general terms we consider that there was a central rhyolite magma body located beneath the caldera. Small volumes of basaltic andesite magma were injected from below and peripherally mixed with the rhyolite magma. There are also significant geochemical variations and differences in modal phenocryst proportions in the intracaldera rhyolite dome lavas to suggest that the central rhyolite magma was compositionally zoned.

It is also considered likely that the central rhyolite magma later started to crystallise and was accompanied by a concentration of volatiles, which led to the reopening of the flanking ring fractures and extrusion of the postcaldera hornblende rhyolites. The Omahine dacite could represent the product derived from the final injection of andesite from below and mixing with residual crystallising rhyolite magma.

The basaltic andesites have similar compositions to the Taupo Volcanic Zone andesites (Cole 1979; Graham & Hackett 1987), and their low Nb and TiO_2 abundances and high Ba/La (23 in sample 15), Ba/Nb, and Ba/Zr ratios are typical of subduction-related magmas (Ewart 1982; Pearce 1983; Thompson et al. 1984). The very high La and Y contents in samples 44, 27, 67, and 16 have been rechecked and are most likely caused by posteruptive surficial weathering or alteration (cf. Nagashima et al. 1986). The basaltic andesites have high Al_2O_3 and Sr abundances and are similar to the Type 2 Ruapehu andesites of Graham & Hackett (1987) except they have lower K_2O and Rb contents. Tunaiti dacites have much lower Sr but higher Zr and Rb than Tauhara dacites (Graham & Worthington 1988), but lower Zr and Rb than Ruapehu dacites (Graham & Hackett 1987). Tunaiti rhyolites have lower Ba, Sr, and Zr abundances but higher K_2O and Rb compared with the average Taupo Volcanic Zone rhyolites of Cole (1979) and Reid (1983).

SUMMARY AND DISCUSSION

The nature and relations of a variety of volcanic and pyroclastic materials and lake sediments in the Whiritoa–Whangamata region, eastern Coromandel, have been interpreted in terms of a caldera facies model. The recognition of this caldera, named the Tunaiti caldera, has been determined mainly from coastal exposures, and is strongly supported by low-altitude, high resolution aeromagnetic intensity surveys (unpubl. data, G. J. Jones pers. comm.). Magnetic intensities sharply delineate a subcircular structure 5 km in diameter, which is transected by the present-day coastline. The Tunaiti caldera is probably Late Miocene and about 7 Ma in age, based on K-Ar ages on other similar rhyolites close to Whangamata.

We anticipate that this combined volcanic, geological, and geophysical approach will identify many other calderas in eastern Coromandel in the future. By analogy with explosive rhyolitic centres elsewhere, namely those in western U.S.A., it is likely that some centres in Coromandel may contain clusters of adjacent and possibly overlapping calderas.

Very limited inland exposures, and rapid and deep erosion of the Tunaiti caldera and associated rocks, prevent any calculations of erupted volumes of magma. However, the Tunaiti and the other recognised calderas of the Coromandel Volcanic Zone (Kapowai, 6 km diameter; Wharekawa, 6 km; Waihi, 7 km) are very much smaller than those in the Taupo Volcanic Zone which average 23 km in diameter (from data compiled in Wilson et al. 1984). This implies, therefore, that the size of the associated magma chambers and volumes of erupted material are likely to be an order of magnitude smaller than those in the Taupo Volcanic Zone. The reasons for the smaller size are uncertain but may be related to the nature of the crust and the relative lack of rifting of the basement, which is characteristic of the Taupo Volcanic Zone (Walcott 1978; Stern & Davey 1987). Rifting and thinning of the continental crust may favour the accumulation of larger volumes of magma at higher crustal levels.

The overall positions of the calderas in eastern Coromandel could be controlled by northeast-trending structures (Fig. 1) associated with the Hauraki Rift (of Hochstein & Nixon 1979) or precursors of the Hauraki Rift. Structural relationships between calderas and cross-faults, referred to as transfer faults or accommodation zones, orientated normal to, or at high angles to major rift structures, are well known in the western U.S.A. (Smith & Luedke 1984; Chapin 1989). For example, the Socorro, Sawmill Canyon-Magdalena, and Mt Withington calderas associated with the Oligocene–Miocene Mogollon-Datil volcanic field are aligned along the Socorro accommodation zone (SAZ), which developed along a pre-Rio Grande rift lineament. This lineament was parallel to the early-rift extension direction and controlled the location and orientation of the accommodation zone (Chapin 1979). Some accommodation zones like the SAZ appear to leak magmas, and the Valles Caldera is possibly a Pleistocene example overlying the intersection of the Rio Grande rift and the Jemez volcanic lineament (Goff et al. 1989).

The rocks associated with the Tunaiti caldera have compositions which have evolved in time from andesites to dacites to rhyolites, but contrasting incompatible element ratios and the large compositional gaps between these rocks indicate that they were not derived from a single evolving magma chamber. Rather, the andesites have been derived from an independent source and periodically mixed with rhyolitic magma to derive the dacites. The andesites have low Nb and TiO_2 abundances and high Ba/La, Ba/Nb, and Ba/Zr ratios typical of subduction-related magmas, and probably ascended through the crust and mixed with upper crustal rhyolitic reservoirs. Eruptives of dacitic composition appear to be volumetrically significant in Tunaiti caldera, which is an important contrast with the calderas in the Taupo Volcanic Zone where dacites are volumetrically smaller and generally confined to flows and domes on the rim or outside of the rhyolitic calderas (Graham & Worthington 1988).

Hot springs and solfataras are characteristic of the terminal stages of caldera cycles (Smith & Bailey 1968), but hydrothermal alteration or mineralisation associated with the Tunaiti caldera has not been observed. It is emphasised that only a narrow cross-section of the caldera can be examined in outcrop along the coast, and that localised zones of hydrothermal alteration associated with the caldera elsewhere must be expected. The close spatial and temporal association of hydrothermal activity, epithermal mineralisation, and caldera volcanism is well known in the Taupo Volcanic Zone, western U.S.A., and many other places, and implies significant economic importance to the recognition of caldera structures in Coromandel. Furthermore, the presence of lake sedimentation penecontemporaneous with volcanism also raises the possibility that lenses of subaqueous, volcanogenic, exhalative, massive sulphide deposits could occur in moat deposits between the caldera rim and the intracaldera rhyolite dome complexes, or beneath the rhyolite domes.

ACKNOWLEDGMENTS

We thank D. J. Lowe and P. R. Moore for useful comments and constructive criticism of an early draft of this paper. Helpful referees' reviews of the manuscript were provided by P. R. Kyle and I. J. Graham. We would also like to thank G. J. and L. P. Jones and Lachlan Pacific N. L. for their cooperation and access to their unpublished aeromagnetic intensity maps. Financial support to R.M.B. from the New Zealand University Grants Committee and the University of Waikato Research Committee is gratefully acknowledged. We would also like to thank K. Palmer of the Analytical Facility, Victoria University of Wellington, for XRF analyses and assistance with microprobing. We are grateful to F. Bailey for draughting the diagrams, and Elaine Norton for typing the manuscript.

REFERENCES

Bailey, R. A.; Dalrymple, G. B.; Lanphere, M. A. 1976: Volcanism, structure, and geochronology of Long Valley Caldera, Mono County, California. *Journal of geophysical research 81*: 725–744.

Cas, R. A. F.; Wright, J. V. 1987: Volcanic successions, modern and ancient. London, Allen & Unwin.

Chapin, C. E. 1989: Volcanism along the Socorro accommodation zone, Rio Grande rift, New Mexico. *In*: Chapin, C. E.; Zidek, J. *ed.* Field excursions to volcanic terranes in the western United States, Vol. 1: Southern Rocky Mountain region. *New Mexico Bureau of Mines and Mineral Resources memoir 46*: 46–57.

Christiansen, R. L. 1979: Cooling units and composite sheets in relation to caldera structure. *In*: Chapin, C. E.; Elston, W. E. *ed.* Ash-flow tuffs. *Geological Society of America special paper 180*: 29–42.

———1984: Yellowstone magmatic evolution: its bearing on understanding large-volume explosive volcanism. *In*: Studies in geophysics. Explosive volcanism: inception, evolution, and hazards. Washington, D.C., National Academy Press. Pp. 84–95.

Cole, J. W. 1979: Structure, petrology and genesis of Cenozoic volcanism, Taupo Volcanic Zone, New Zealand—a review. *New Zealand journal of geology and geophysics 22*: 631–657.

Doell, R. R.; Dalrymple, G. B.; Smith, R. L.; Bailey, R. A. 1968: Paleomagnetism, potassium-argon ages, and geology of rhyolites and associated rocks of the Valles Caldera, New Mexico. *Geological Society of America memoir 116*: 211–248.

Ewart, A. 1982: The mineralogy and petrology of Tertiary – Recent orogenic volcanic rocks: with special reference to the andesitic-basaltic compositional range. *In*: Thorpe, R.S. *ed.* Andesites. Chichester, Wiley. Pp. 25–95.

Fulton, B. W. J. 1988: The volcanic geology of the Whiritoa–Whangamata area. Unpublished M.Sc. thesis, lodged in the Library, University of Waikato, Hamilton.

Goff, F.; Gardner, J. N.; Baldridge, W. S.; Hulen, J. B.; Nielson, D. L.; Vaniman, D.; Heiken, G.; Dungan, M. A.; Broxton, D. 1989: Volcanic and hydrothermal evolution of Valles caldera and Jemez volcanic field. *In:* Chapin, C. E.; Zidek, J. *ed.* Field excursions to volcanic terranes in the western United States, Vol. 1: Southern Rocky Mountain region. *New Mexico Bureau of Mines and Mineral Resources memoir 46*: 381–434.

Graham, I. J.; Hackett, W. R. 1987: Petrology of calc-alkaline lavas from Ruapehu Volcano and related vents, Taupo Volcanic Zone, New Zealand. *Journal of petrology 28*: 531–567.

Graham, I. J.; Worthington, T. J. 1988: Petrogenesis of Tauhara dacite (Taupo Volcanic Zone, New Zealand)—evidence for magma mixing between high-alumina andesite and rhyolite. *Journal of volcanology and geothermal research 35*: 279–294.

Hochstein, M. P.; Nixon, I. M. 1979: Geophysical study of the Hauraki Depression, North Island, New Zealand. *New Zealand journal of geology and geophysics 22*: 1–19.

Hogg, A. G.; McCraw, J. D. 1983: Late Quaternary tephras of Coromandel Peninsula, North Island, New Zealand: a mixed peralkaline and calcalkaline tephra sequence. *New Zealand journal of geology and geophysics 26*: 163–187.

Hunt, T. M.; Syms, M. C. 1977: Sheet 3—Auckland. Magnetic map of New Zealand 1 : 250 000. Total force anomalies. Wellington, Department of Scientific and Industrial Research.

Lipman, P. W. 1975: Evolution of the Platoro caldera complex and related volcanic rocks, southeastern San Juan Mountains, Colorado. *United States Geological Survey professional paper 852*: 128 p.

———1976: Caldera-collapse breccias in the western San Juan Mountains, Colorado. *Geological Society of America bulletin 87*: 1397–1410.

———1984: The roots of ash flow calderas in western North America: windows into the tops of granitic batholiths. *Journal of geophysical research 89*: 8801–8841.

Moore, P. R. 1983: Rhyolite domes and pyroclastic rocks (Whitianga Group) of the Hahei area, Coromandel Peninsula. *Journal of the Royal Society of New Zealand 13*: 79–92.

Nagashima, K.; Miyawaki, R.; Takase, J.; Nakai, I.; Sakurai, K.; Matsubara, S.; Kato, A.; Iwano, S. 1986: Kimuraite, $CaY_2(CO_3)_4 \cdot 6H_2O$, a new mineral from fissures in an alkali olivine basalt from Saga Prefecture, Japan, and new data on lokkaite. *American mineralogist 72*: 1028–1033.

Pearce, J. A. 1983: Role of the sub-continental lithosphere in magma genesis at active continental margins. *In*: Hawkesworth, C. J.; Norry, M. J. *ed.* Continental basalts and mantle xenoliths. Nantwich, United Kingdom, Shiva Publishing Ltd. Pp. 230–249.

Peccerillo, A.; Taylor, S. R. 1976: Geochemistry of Eocene calc-alkaline volcanic rocks from the Kastamonu area, northern Turkey. *Contributions to mineralogy and petrology 58*: 63–81.

Ratté, J. C.; Steven, T. A. 1967: Ash flows and related volcanic rocks associated with the Creede Caldera, San Juan Mountains, Colorado. *United States Geological Survey professional paper 524-H*: H–H58.

Reid, F. 1983: Origin of the rhyolitic rocks of the Taupo Volcanic Zone, New Zealand. *Journal of volcanology and geothermal research 15*: 315–338.

Rogan, M. 1982: A geophysical study of the Taupo Volcanic Zone, New Zealand. *Journal of geophysical research 87*: 4073–4088.

Rutherford, N. F. 1976: Petrochemistry of ignimbrites from the central North Island and Coromandel, New Zealand. Unpublished Ph.D. thesis, lodged in the Library, University of Auckland, Auckland.

———1978: Fission-track age and trace element geochemistry of some Minden Rhyolite obsidians. *New Zealand journal of geology and geophysics 21*: 443–448.

Sakuyama, M. 1979: Evidence of magma mixing: petrological study of Shirouma-Oike calc-alkaline andesite volcano, Japan. *Journal of volcanology and geothermal research 5*: 179–208.

Seward, D.; Moore, P. R. 1987: New fission track ages for some Minden Rhyolites (Whitianga Group), eastern Coromandel Peninsula. *New Zealand Geological Survey record 20*: 105–109.

Skinner, D. N. B. 1986: Neogene volcanism of the Hauraki Volcanic Region. *In*: Smith, I. E. M. *ed.* Late Cenozoic volcanism in New Zealand. *The Royal Society of New Zealand bulletin 23*: 21–47.

Smith, R. L.; Bailey, R. A. 1968: Resurgent cauldrons. *Geological Society of America memoir 116*: 613–662.

Smith, R. L.; Luedke, R. G. 1984: Potentially active volcanic lineaments and loci in western conterminous United States. *In*: Studies in geophysics. Explosive volcanism: inception, evolution, and hazards. Washington, D.C., National Academy Press. Pp. 47–66.

Smith, R. L.; Bailey, R. A.; Ross, C. S. 1961: Structural evolution of the Valles Caldera, New Mexico, and its bearing on the emplacement of ring dikes. *United States Geological Survey professional paper 424-D*: D145–D149.

Spencer, K. H.; Lindsley, D. H. 1981: A solution model for coexisting iron-titanium oxides. *American mineralogist 66*: 1189–1201.

Stern, T. A.; Davey, F. J. 1987: A seismic investigation of the crustal and upper mantle structure within the Central Volcanic Region of New Zealand. *New Zealand journal of geology and geophysics 30*: 217–231.

Stormer, J. C. 1982: The recalculation of multicomponent Fe-Ti oxide analyses for geothermometry: a quasi-thermodynamic model. *EOS 63 (2)*: 471.

Thompson, R. N.; Morrison, M. A.; Hendry, G. L.; Parry, S. J. 1984: An assessment of the relative roles of crust and mantle in magma genesis: an elemental approach. *Philosophical transactions of the Royal Society of London A310*: 549–590.

Walcott, R. I. 1978: Tectonics and late Cenozoic evolution of New Zealand. *Geophysical journal of the Royal Astronomical Society 52*: 137–164.

Wilson, C. J. N.; Rogan, A. M.; Smith, I. E. M.; Northey, D. J.; Nairn, I. A.; Houghton, B. F. 1984: Caldera volcanoes of the Taupo Volcanic Zone, New Zealand. *Journal of geophysical research 89*: 8463–8484.

Woodward, D. J. 1971: Sheet 3—Auckland. Gravity map of New Zealand 1 : 250 000. Isostatic and Bouguer anomalies. Wellington, Department of Scientific and Industrial Research.